JOURNAL OF Applied Polymer SCIENCE

A New Liquid Rubber-Assisted Dispersion of Organoclay in Carbon Black Filled Carboxylated Acrylonitrile–Butadiene Rubber Matrix

Praveen Sreenivasan, Debdatta Ratna, Pradeesh Albert,* Jayendran Somashekaran, Rohidas Raut, Bikash Chandra Chakraborty

Naval Materials Research Laboratory, Shil-Badlapur Road, Anandnagar, Mumbai 421506, Maharashtra, India

*Present address: Naval Physical and Oceanographic Laboratory, Thrikakkara, Kochi 682 021, India

Correspondence to: P. Sreenivasan (E-mail: praveens76@gmail.com)

ABSTRACT: A novel route for the preparation of rubber–carbon black–nanoclay (NC) nanocomposites with XNBR as a matrix and a carboxyl-terminated copolymer of butadiene and acrylonitrile (CTBN) as a low-molecular-weight modifier for commercially available NC is presented in this article. The addition of NC to the rubber (after the NC was mixed with CTBN in a 2 : 1 ratio) showed remarkable improvement in the mechanical properties. The clay loading was varied from 0 to 10 parts per hundred rubber (phr). An amount of 20 phr N330 black was incorporated into all of the formulations. The properties were compared with those of a control XNBR compound having only 20 phr N330. X-ray diffraction revealed a combination of a high level of intercalated and exfoliated structures in such nanocomposites. Transmission electron microscopy confirmed the improvement in dispersion as a result of addition of CTBN. A 127% increase in the tensile strength and a 53% increase in the elongation at break were achieved. © 2012 Wiley Periodicals, Inc. J. Appl. Polym. Sci. 000: 000–000, 2012

KEYWORDS: dispersions; microscopy; nanocomposites; rubber; WAXS

Received 28 January 2012; accepted 21 June 2012; published online

DOI: 10.1002/app.38256

INTRODUCTION

In the rubber industry, rubbers are mixed with different ingredients to improve their processing and properties, including their tear strength, abrasion resistance, and aging behavior. Carbon black is an important ingredient and is used extensively to improve the mechanical properties and hardness of rubber vulcanizates. Even though the use of carbon black is needed to attain the final properties in rubber compounds, ever-increasing crude oil prices and pollution concerns have forced both those in industry and researchers to find ways to minimize the use of this filler. One such approach is the development of rubber–carbon black–nanoclay (NC) hybrid nanocomposites, which allows a substantial reduction in the carbon black loading.

Polymer nanocomposites have drawn considerable attention in recent years. Advances in research on polymer nanocomposites and in the field of rubber/layered silicate nanocomposites elaborating their production methods, curing characteristics, mechanical properties, and morphology have been reviewed recently by various researchers. Ratna[1,2] discussed in detail the advantages of thermoset-resin-based NC composites. The methods of making thermoset nanocomposites discussed include the preintercalation of the layered silicate by swelling in the resin for a period of time before curing, followed by the addition of a suitable curing agent and crosslinking. Sonication is used in many cases to break the tactoids. The reinforcement is more prominent in rubbery thermosets compared to glassy thermosets. The incorporation of 15 wt % clay into a rubbery epoxy resulted in about an 800% increase in the tensile strength. Jordan et al.[3] and Ray[4] reviewed recent works on polymer matrix nanocomposites. An overview of the processing techniques, including melt blending, *in situ* polymerization, and solution blending, were discussed. The melt mixing route produced good, reasonably well-dispersed samples at lower filler volume fractions (i.e., 4.8 and 9.2%), but aggregation was found at a higher volume fraction (13.2%). The solution method produced samples without aggregation and, in addition, greatly increased the particle–polymer matrix interfacial interaction. The *in situ* polymerization technique produced well-dispersed samples when the inclusions were around 50 nm in size, but aggregation occurred for smaller particles around 12 nm in size. For all systems, the elastic modulus increased with increasing volume fraction of the inclusions. For the smaller weight fraction (2%), the increase in effective elastic modulus was 40% over the modulus of the pure polymer system. Vu et al.[5] studied the clay nanolayer reinforcement of cis-1,4-polyisoprene with melt mixing in a standard internal

mixer. The properties of the nanocomposites were compared with that of compounds with similar loadings of silica filler. A 10-phr NC loading resulted in a tensile strength of 17 MPa, as compared to 5.2 MPa for a similar loading of silica. Sadhu and Bhomick[6,7] reported the effect of the chain length of amine, the loading of clay, and the type of curing system on styrene–butadiene rubber (SBR)–clay nanocomposites. An increase in the tensile strength from 1.2 MPa (for gum rubber vulcanizate) to 3.4 MPa and an increase in the elongation at break from 111 to 347% were reported for SBR loaded with 16 phr NC. With increasing chain length of the amine, there was an increase in the tensile strength. The peroxide and sulfur curing systems displayed similar strength, but higher elongation and slightly lower modulus values were obtained with the sulfur curing system. Karger-Kocsis et al.[8] published a survey on the recent achievements with thermoset rubber/layered silicate nanocomposites. The authors attributed the phenomenon of unusual increases in the elongation at break values observed in rubber nanocomposites with increases in the NC loading to the encapsulation of individual clay layers and tactoids in a more crosslinked rubber fraction than the bulk itself. As a result, the less crosslinked portion of the rubber contributed more toward the deformation of the rubber matrix; this resulted in a higher percentage in the elongation at break. Wu et al.[9] studied the effects of the characteristics of rubber, mixing, and vulcanization on the structure and properties of rubber–clay nanocomposites prepared by melt blending. The authors ascribed an increase in tensile strength of four to five times for rubber nanocomposites compared to the pure rubber vulcanizate to the slippage of the rubber molecules and the orientation of the intercalated NC. Paul and Robeson[10] detailed the technology involved with exfoliated clay-based nanocomposites and the mechanism of organoclay dispersion and exfoliation during the melt process, illustrating the different states of dispersion of organoclay in the polymers.

Bhowmick et al.[11] studied the effect of carbon black on the properties of rubber–clay nanocomposites. In our previous studies with black-filled SBR–NC composites, we observed the formation of unique nanounits between the clay platelets and carbon black particles, which led to a synergistic effect in the improvement of the physical properties of rubber nanocomposites.[12] Very recently, Praveen et al.[13] investigated the effect of the rubber Mooney viscosity and polarity on the morphology and the physical properties of millable polyurethane and bromobutyl rubber–clay nanocomposites. They reported that the addition of NC into the rubber led to significant improvements in the mechanical and barrier properties.

A through literature survey revealed that there are fewer research reports on rubber–nanocomposites than on thermoplastic- and thermoset-resin-based nanocomposites.[14–18] Rubber should be the preferred polymer matrix in the production of nanocomposites because of the following facts. First, amine compounds (used as low-molecular-weight intercalants/surfactants in organophilic layered silicates) act in sulfur-curing rubber recipes as activators.[19] Thus, layered silicates intercalated by amine compounds (containing primary, tertiary, and quaternary amines) may be involved in the sulfur-curing reactions. Second, rubbers are high-molecular-weight polymers that show extremely high viscosities during melt compounding. Because of this, high shear stresses may act locally on the layered silicate stacks and cause them to shear and peel apart and, thus, delaminate.[8]

To incorporate layered silicates in rubbers, the following routes are usually followed: solution blending (solvent-assisted techniques),[20–22] latex compounding (water-assisted techniques),[23,24] and melt mixing (direct methods).[25] The drawbacks of a solution intercalation method are the requirement of suitable monomer–solvent or polymer–solvent pairs, and the high costs associated with the solvents, their disposal, and their impact on the environment. Melt intercalation does not require the use of any solvent. The melt-intercalation process involves the annealing of a mixture of the polymer and organically modified NC above the softening point of the polymers under shear. During annealing, the polymer chains diffuse from the bulk polymer melt into the galleries between the silicate layers; this leads to the formation of nanocomposites. This method has become the mainstream for the fabrication of polymer nanocomposites in recent years because it is simple, economical, environmentally friendly, and easy to implement in current polymer processing techniques. However, during the processing of rubber in a two-roll mill, the high shear rate is accompanied by a significant compressive force; this leads to layer collapse in the NC. This was highlighted in our recent X-ray diffraction (XRD) studies on SBR nanocomposites.[12] In addition to the processing difficulties, the very high molecular weight of rubbers makes it difficult for the rubber molecules to intercalate into the clay galleries. As a result, the nanoparticle dispersion is affected and leads to clay agglomeration.

In this work, we report a novel approach for the preparation of elastomer nanocomposites with a low-molecular-weight liquid rubber [carboxyl-terminated copolymer of butadiene and acrylonitrile (CTBN)] as a physical modifier for organically modified clay. Here, unlike in the usual method of mixing NC into rubber (through direct addition of the NC into a two-roll mill after the mastication of rubber), the NC was first mixed with the CTBN in an internal mixer to form a CTBN–NC master batch. The resulting master batch was then added to the masticated rubber in a two-roll mill; this was followed by the addition of carbon black and the vulcanizing agents. With CTBN used as a physical modifier, the clay layers were expected to form intercalated and exfoliated structures before the final addition into the high-molecular-weight carboxylated acrylonitrile butadiene rubber (XNBR) matrix. CTBN, being oligomeric in nature, easily intercalated into the clay gallery. Once the CTBN intercalation took place, the hydrophobicity of the gallery increased, and the intercalation of high-molecular-weight rubber was favored. Unlike conventional organomodification of clay,[17] this method did not involve any ion exchange of cations (located inside the clay galleries) with organic cations such as alkylammoniums to increase the layer spacing. The mechanism involved in this novel technique was the peeling apart of commercial organomodified clay platelets[10] by CTBN in a combined diffusion and shear process. The similar molecular structure of that of CTBN to that of XNBR ensured faster diffusion of the polymer molecules into the rubber matrix and the attainment of a uniform cure in the final vulcanizate. This process was

Table I. Rubber Formulation

Ingredient	XHAF 20	XCT 2.5	XCT 5	XNC2.5	XNC5	XNC10	XNC-CT 2.5	XNC-CT 5	XNC-CT 10
XNBR	100	100	100	100	100	100	100	100	100
Zinc oxide	3	3	3	3	3	3	3	3	3
Stearic acid	2	2	2	2	2	2	2	2	2
TDQ	1	1	1	1	1	1	1	1	1
NC	0	0	0	2.5	5	10	2.5	5	10
CTBN	0	2.5	5	0	0	0	1.25	2.5	5
HAF	20	20	20	20	20	20	20	20	20
DOP	2	2	2	2	2	2	2	2	2
CBS	1.5	1.5	1.5	1.5	1.5	1.5	1.5	1.5	1.5
Sulfur	2	2	2	2	2	2	2	2	2
PVI	0.1	0.1	0.1	0.1	0.1	0.1	0.1	0.1	0.1

TDQ, trimethyl diqunoline; DOP, dioctyl phthalate; CBS, Cyclohexyl Benzothiazol Sulfenamide; PVI, prevulcanization inhibitor.

expected to minimize the layer collapse in the clay galleries and ensure the maximum utilization of the NC added into the matrix.

EXPERIMENTAL

Materials Used

Krynac X 146 carboxylated butadiene–acrylonitrile terpolymer [Mooney viscosity ML(1+4)100°C 45 ± 5 Mooney units (MU) and acrylonitrile content = 32.5 ± 1.5%] was procured from Lanxess (Thane, Mumbai, India). Nanomer I30E, organically modified montmorillonite clay modified with octadecyl amine (mean dry particle size 8–10 μm + 325-mesh residue, specific gravity = 1.71, minimum mineral purity = 98.5%) was procured from Nanocor, Inc. Hoffman Estates, IL USA. High-abrasion furnace black [HAF (N330), iodine absorption number = 82 ± 7 g/kg, dibutyl phthalate (DBP) absorption number = 102 ± 7 m^3/kg, nitrogen absorption specific area = 103 m^2/kg) was procured from Philips Carbon Black, Ltd. Kolkatta, West Bengal, India. CTBN 1300 × 13 (acrylonitrile content = 26%, number-average molecular weight = 3150, specific gravity = 0.96 at 25°C) was procured from Emerald Speciality polymers, Emerling Avenue Akron, OH, USA. The other rubber chemicals were analytical grade and were purchased from local suppliers.

Preparation of the XNBR Nanocomposites

The mixing of XNBR and NC was done by the adoption of two separate processes. In first process (method 1), the NC was incorporated directly into the rubber matrix in a two-roll mill. The incorporation was done in the initial stages of the mixing, before the addition of other fillers. In the second process (method 2), NC was mixed with CTBN at a selected ratio to form a semisolid dough. In all cases, the ratio of NC to CTBN was maintained at 2 : 1. The idea was to use a minimum amount of CTBN in the process. However, when CTBN was added at levels below the previously mentioned quantity, the complete wetting of NC was not possible. The mixing was done at 70°C for 5–7 min in an internal mixer at a speed of 50 rpm. The dough was then added to the rubber matrix with the procedure used in method 1. In both methods, 2.5, 5, and 10 phr clay loadings were used. A loading of 20 phr N330 carbon black was also added to all of the compositions. After the NC addition, the compound was passed through a tight nip (<1 mm) three to four times. The optimum cure time (OCT) was determined at 150°C with a moving die rheometer (MDR 2000, Alpha technologies, Akron, Ohio, USA). The samples were molded in the form of sheets by compression molding at 150°C at their respective OCTs. The base rubber formulation used in this study is given Table I. Table II reports the various designations used for the compositions prepared in this investigation.

Wide-Angle X-Ray Diffraction (WAXD) Studies of the Nanocomposites

WAXD at a lower angular range was used to study the nature and dispersions of the clay in the filled samples. The XRD patterns were obtained with a high-resolution X-ray diffractometer (X'Pert Pro, PANalytical) with monochromatic Cu Kα radiation (wavelength = 1.542 Å) at a θ scan rate of 1°/min in the range 2–10°. An acceleration voltage of 40 kV and a beam current of 30 mA were used. The *d*-spacing of the clay particles were calculated with Bragg's law. The samples used for XRD were flat test pieces cut from molded sheets. To conduct the XRD of the CTBN–NC masterbatch, the master batch was passed between the rolls of a two-roll mill to obtain a flat test piece.

Table II. Nanocomposite Designations

Compound name	Composition
XNBR-HAF 20	XNBR + 20 phr HAF
XCT 2.5	XNBR + 20 phr HAF + 2.5 phr CTBN
XCT 5	XNBR + 20 phr HAF + 5 phr CTBN
XNC 2.5	XNBR + 20 phr HAF + 2.5 phr NC
XNC 5	XNBR + 20 phr HAF + 5 phr NC
XNC 10	XNBR + 20 phr HAF + 10 phr NC
XNC-CT 2.5	XNBR + 20 phr HAF + 2.5 phr NC + 1.25 phr CTBN
XNC-CT 5	XNBR + 20 phr HAF + 5 phr NC + 2.5 phr CTBN
XNC-CT 10	XNBR + 20 phr HAF + 10 NC + 5 phr CTBN

Table III. Curing Characteristics of the XNBR Nanocomposites

Composition	Scorch time (min)	OCT (min)	M_H (kg cm)
XNBR-HAF 20	9.8	23.5	15.3
XCT 2.5	10	24.1	16.6
XCT 5	10.1	26.0	12.8
XNC 2.5	9.1	22.5	16.9
XNC 5	8.5	20.3	19.6
XNC 10	7.6	17.9	17.6
XNC-CT 2.5	4.9	12.0	15.0
XNC-CT 5	4.6	11.3	14.4
XNC-CT 10	4.3	11.8	13.3

Transmission Electron Microscopy (TEM) Analysis

A JEOL (Tokyo, Japan) JEM-2100 transmission electron microscope with a lanthanum hexaborate filament was used (acceleration voltage = 200 kV, beam current = 116 μA) to observe the morphology of the XNBR nanocomposites. Samples were cut to 50 nm thin sections with a Leica Ultracut ultracryotome at −60°C. The cut samples were supported on a copper mesh before observation under a microscope.

Mechanical Properties

Tensile specimens were punched out from the molded sheets with an ASTM Die-C. The tests were carried out as per ASTM D-412 in a universal testing machine (Hounsfield 50K, Salfords, Surrey, England) at a crosshead speed of 500 mm/min. The tensile properties reported here are the average values from five samples.

Dynamic Mechanical Properties

Dynamic mechanical thermal analysis was conducted with rectangular samples with dimensions of 30 mm (L) × 10 mm (W) × 2 mm thickness on a dynamic mechanical analysis machine from GABO Ahlden (DE), Germany. A dynamic temperature sweep test was conducted at a frequency of 1 Hz and a strain of 0.05% strain, with a temperature range of −80 to +50°C at a heating rate of 2°C/min. A dynamic strain sweep test was conducted at a frequency of 1 Hz at ambient temperature.

RESULTS AND DISCUSSION

Curing Characteristics

The curing characteristics of the rubber nanocomposites were studied with the moving die rheometer at 150°C. The individual and combined effects of NC and CTBN on the curing time and maximum torque (M_H) of XNBR/HAF were studied. The respective curing times and M_H values are given in Table III.

Effects of CTBN. The effects of the addition of CTBN on the curing characteristics of the XNBR/HAF matrix are depicted in Figure 1. The addition of only CTBN to the rubber–carbon black matrix led to increases in the cure times compared to those of the control XNBR with 20phr high abrasion furnace black (HAF) (XHAF 20). This may have been due to the fact that with the addition of CTBN, the actual curative level present in the XNBR matrix was diluted because of the increase in the unsaturation level in the compound. The maximum rheometer torque values decreased when the CTBN loading was increased from 2.5 to 5 phr. This could be explained by the dual effects of CTBN occurring simultaneously. The addition of CTBN improved the dispersion and resulted in a higher torque, whereas the plasticizing effect of CTBN tended to reduce the torque. At lower loadings of CTBN (≤2.5 phr), the first factor predominated, whereas at a higher loading of CTBN (>2.5 phr), the second factor predominated. This explained the existence of an optimum value of CTBN concentration for obtaining higher physical properties.

Effects of NC. The effects of NC on the curing characteristics of the XNBR/HAF matrix are shown in Figure 2. The addition of NC to the rubber matrix lead to steady decreases in the scorch time and OCT. There were decreases of 55% in the scorch time and 51% in OCT compared to the control XNBR/HAF. This could be explained by consideration of the mechanism of accelerated sulfur vulcanization in rubbers.[16–18] Amine compounds (used as low-molecular-weight intercalants/surfactants in organophilic layered silicates) act as activators in sulfur-curing rubber recipes.[13,14] Thus, layered silicates intercalated by amine compounds (containing primary, tertiary, and quaternary amines) may have been involved in the sulfur-curing reactions, activating the curing process and, thereby, decreasing the curing time. However, the M_H values increased as the loading of NC was increased from 2.5 to 5 phr. The further addition of NC

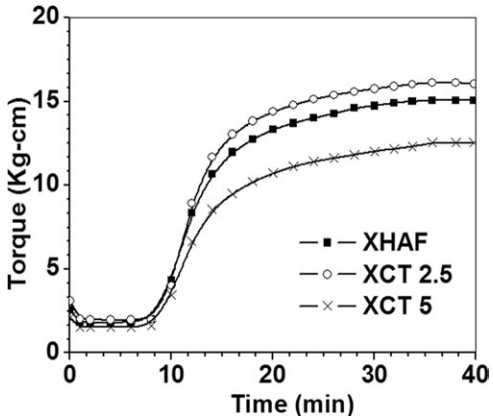

Figure 1. Rheometer curves for XNBR with carbon black and CTBN.

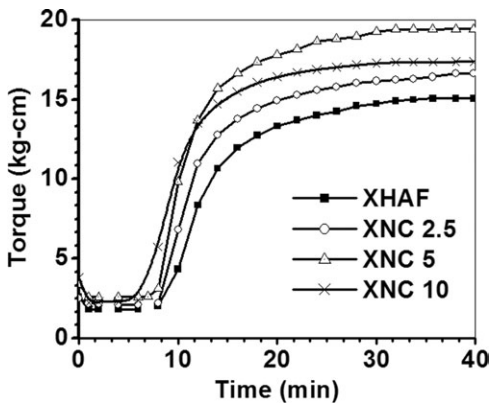

Figure 2. Rheometer curves for XNBR with carbon black and NC.

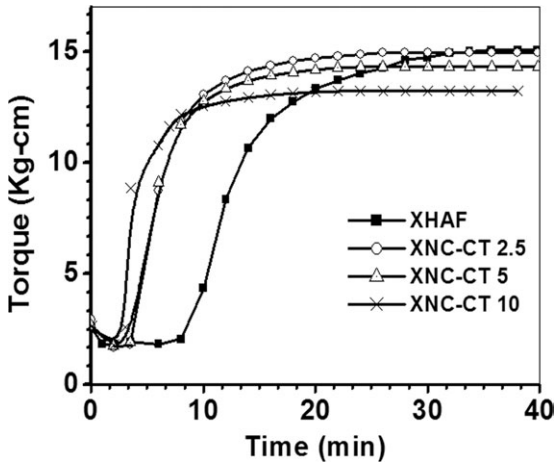

Figure 3. Rheometer curves for XNBR with carbon black and CTBN-modified NC.

(10 phr) led to a decrease in M_H values. The M_H value of a compound is an indication of the degree of curing attained in a vulcanizate and the nature of the polymer–filler and filler–filler interactions in a cured compound. The results, thus, show that the 5-phr NC provided the optimum polymer–filler interactions, and further increases in the NC loading led to filler agglomeration and weak filler–filler interactions.[26]

Effects of CTBN-Modified NC. When NC was modified with CTBN and added to the rubber, the difference in M_H attained diminished, and the curing times remained the same for all of the nanocomposites. This effect on the curing behavior was attributed to the neutralization of the opposite individual effects of CTBN and NC on the nanocomposite curing chemistry discussed previously. The curing characteristics are shown in Figure 3. XNC (XNBR rubber with Nanaoclay)–CT 2.5, with the lowest CTBN and NC contents, showed the highest torque values in this series. XNC–CT 10 showed the lowest torque values, which was expected because its higher amount of low-molecular-weight CTBN content acted as a plasticizer.

WAXD Studies

A polymer nanocomposite, in general, has three types of morphology: immiscible (conventional or microcomposite), intercalated, and miscible or exfoliated.[10] In immiscible morphologies, the organoclay platelets exist in particles comprised of tactoids or aggregates of tactoids, more or less as they were in the organoclay powder. Thus, the wide-angle X-ray scan of the polymer composite was expected to look essentially the same as that obtained for the organoclay powder; there is no shifting of the X-ray *d*-spacing. In the case of intercalated nanocomposites, often the X-ray scans of polymer nanocomposites show a peak reminiscent of the organoclay peak but shifted to a lower 2θ or larger *d*-spacing. The fact that there is a peak indicates that the platelets are not exfoliated. The peak shift indicates that the gallery has expanded, and it is usually assumed that polymer chains have entered or have been intercalated into the gallery. It is possible that the gallery expansion may, in some cases, be caused by the intercalation of oligomers or low-molecular-weight polymer chains. The polymer–clay intercalation would be useful and may be considered as a precursor to exfoliation. For completely exfoliated organoclay, no wide-angle X-ray peak is expected for the nanocomposite because there is no regular spacing of the platelets, and the distances between platelets would, in any case, be larger than what wide-angle X-ray scattering can detect.[10]

The XRD scans of the organoclay and black-filled XNBR nanocomposites with only organoclay are shown in Figure 4. The clay shows the d_{100} peak at $2\theta = 3.9$ (Figure 4 inset), which corresponded to a *d*-spacing of 2.26 nm. This indicated that modification of the clay with organic ions not only made the clay surface hydrophobic but resulted in a tremendous increase in the *d*-spacing (*d*-spacing for untreated clay < 1 nm); this facilitated the penetration of liquid resin into the interlayer galleries.[27] For the nanocomposites prepared by method 1, the d_{001} peak corresponding to pristine organoclay shifted to a higher angle, corresponding to a *d*-spacing of 1.5 nm; this was lower than that of pristine organoclay. Generally, in the case of intercalated nanocomposites, the peak appears at a lower angle and corresponds to a higher *d*-spacing. However, this unusual behavior was also reported by Karger-Kocsis and Wu.[8] They attributed the higher angle shifts in the XRD peaks to the partial removal (extraction) of the amine compound from the intergallery region, which might have contributed to the complex formation (during vulcanization) and led to the collapse of that portion of the organoclay. In our previous studies with SBR–carbon black–NC composites,[12] a similar trend in the XRD scans was reported. This was attributed to the collapsing of clay layers due to the high compressive stress occurring during two-roll mill processing.

Figure 5 shows the XRD scans for CTBN-modified NC. A typical pattern of intercalated morphology, as discussed previously, was observed. The shift in the diffraction peak (found in the case of NC powder) toward lower angles indicated the expansion of clay layers due to the penetration of CTBN molecules in the clay galleries. It was clear that the CTBN modification of NC led to an increase in the wetting of NC by the high-molecular-weight rubber molecules during mixing. Enhanced wetting aided in the transfer of more peeling shear stress on the clay layers and eventually leading to complete layer separation.

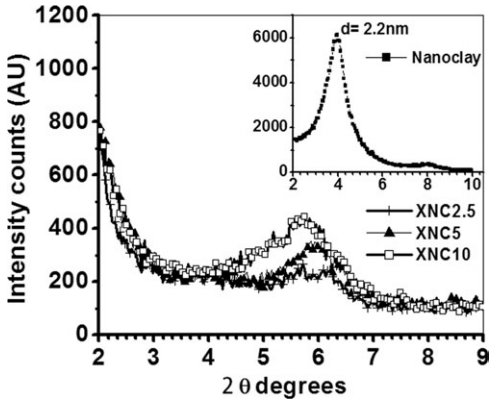

Figure 4. XRD pattern of XNBR with only NC.

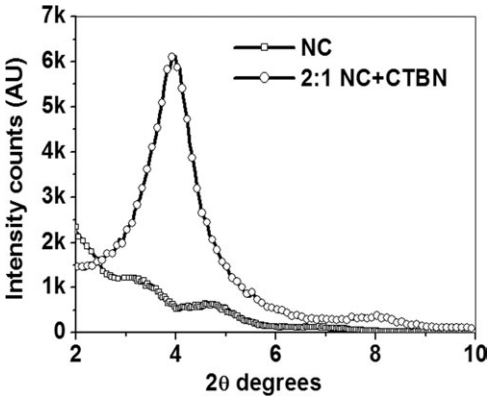

Figure 5. XRD pattern of CTBN-modified NC.

In the case of nanocomposites made by method 2 (XNC–CT 2.5 and XNC–CT 5; Figure 6), no peaks were observed in the aforementioned regions. The absence of a d_{001} peak is generally attributed to exfoliation. In the case of XNC–CT 10, a low intensity broad peak was observed; this suggested the formation of a mixed morphology of intercalated and exfoliated clay structures. It may also be noted that the higher angle shift observed (Figure 4) in the case of the nanocomposites prepared by method 1 was absent in the case of those prepared by method 2. This confirmed the absence of layer collapse under the high compressive force experienced during mixing. However, it was necessary to ascertain the exfoliation by TEM. The TEM results, showing the evidence of exfoliation, are discussed shortly.

Figure 7 illustrates the schematic representation of the different states of dispersion of organoclay in the rubber nanocomposite formation in the presence of CTBN. CTBN, being oligomeric in nature, intercalated easily into the clay galleries. Once the CTBN intercalation took place, the hydrophobicity of the gallery increased; this led to better wetting and the subsequent intercalation of high-molecular-weight rubber. If the polymers and organoclay had increased contact with each other, the stresses imposed during melt mixing broke up aggregates more effectively and sheared the stack into smaller ones by peeling the platelets from these stacks one by one until, given enough time in the mixing device, all the platelets were individually dispersed.

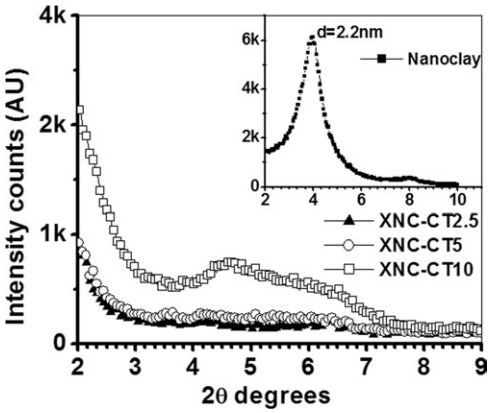

Figure 6. XRD pattern of XNBR with CTBN-modified NC.

Morphology Studies with TEM. To get better insight into the nanocomposites structure, selected samples were characterized by TEM. TEM photomicrographs for the rubber nanocomposites with 5 phr NC without carbon black, prepared with both methods 1 and 2, are present in Figure 8(a,b), respectively. The TEM photomicrographs of the respective black-filled nanocomposites are shown in Figure 9(a,b). It was clear that the nanocomposites prepared by method 1 (without CTBN) showed the presence of clay tactoids with limited intercalation. On the other hand, the same nanocomposite made with CTBN (method 2) showed a mixed morphology of intercalated and exfoliated NC layers in the XNBR matrix. This clearly demonstrated the role of CTBN in improving the dispersion of NC in the rubber matrix.

Mechanical Properties

The tensile properties of the rubber nanocomposites are presented in Table IV. The individual and combined effects of the ingredients (CTBN and NC) on the tensile properties of the XNBR–carbon black matrix are discussed later.

Effects of CTBN. The addition of CTBN to the control XHAF 20 compound resulted in significant increases in the tensile strength and elongation at break compared to those of XHAF 20 alone, as shown in Table IV. The rubber compounds XCT 2.5 and XCT 5, which had only CTBN in the rubber–carbon black matrix, showed tensile strengths of 17.5 and 18.5 MPa, respectively, compared XHAF 20 (tensile strength = 10.6 MPa). XCT 2.5 showed the highest modulus (stress value at 300% elongation) value (7.8 MPa), which decreased as the CTBN loading was increased. This could be explained by consideration of the dual role of CTBN, as discussed previously. CTBN, being an oligomer, acted as a plasticizer/processing aid during the time of carbon black addition; its addition resulted in better dispersion of the carbon black in the rubber. The better dispersion of the carbon black led to a higher tensile strength. As the CTBN content was increased, the plasticizing effect predominated over the reinforcing effect and resulted in a decrease in the modulus and an increase in the elongation at break.

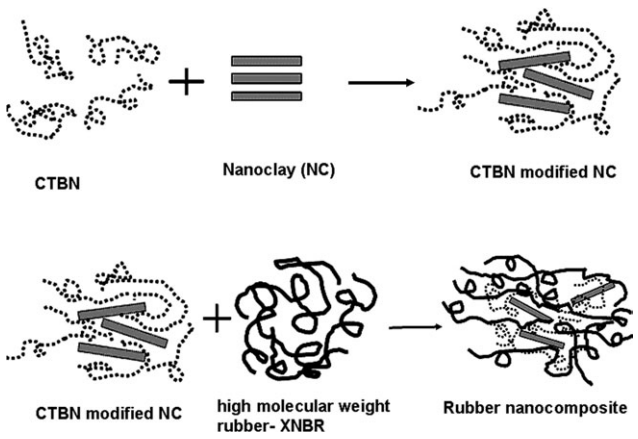

Figure 7. Illustration of the different states of dispersion of the organoclay in the rubber nanocomposite preparation.

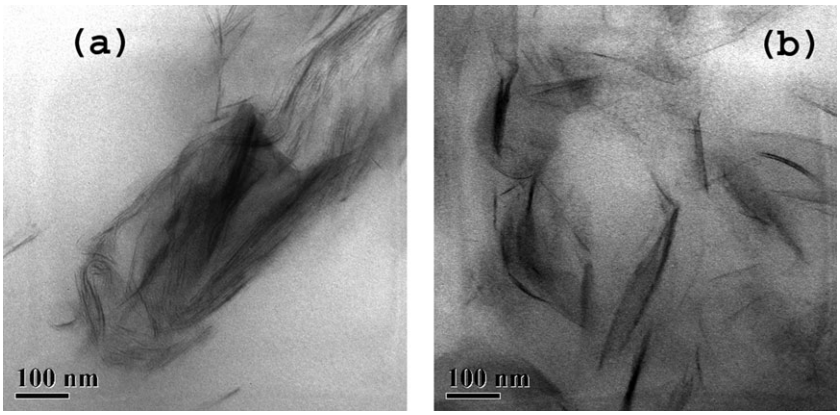

Figure 8. TEM photomicrographs of the XNBR nanocomposites (nonblack compound) (a) with only NC and (b) with CTBN-modified NC.

Effects of NC. NC was added to XHAF 20 in the range of 2.5–10 phr. As depicted in Table IV, the tensile strength of XHAF 20 increased with the addition of 2.5 phr NC. XNC 2.5 showed the maximum tensile strength and elongation at break. The increase in strength was attributed to the synergistic effect between carbon black and NC.[12] In general, an increase in reinforcement is associated with a decrease in ultimate elongation. However, this is not always the case with organoclay-modified rubbers. Karger-Kocsis and Wu[8] speculated that the unexpectedly high elongation in rubber nanocomposites is likely due to the encapsulation of individual clay layers and tactoids in a more crosslinked rubber fraction than the bulk itself. As a result, the less crosslinked portion of rubber contributes more toward the deformation of the rubber matrix and results in a higher percentage of elongation at break.

As the NC loading was increased from 2.5 to 10 phr, the tensile strength and elongation at break decreased. This trend was similar to that of the M_H values observed in the curing studies discussed earlier. The strength decreased due to the agglomeration of NC platelets, which formed weak points in the matrix. The TEM photomicrographs [Figure 8(a)] clearly show the formation of NC agglomerates.

Effects of the CTBN-Modified NC. The reinforcing effect of NC increased tremendously after the modification with CTBN. In contrast to the nanocomposites made by method 1 (without CTBN), the composites made by method 2 showed a higher reinforcement (Table IV). XNC–CT 5 showed a maximum tensile strength and elongation at break of 24.8 MPa and of 574%, respectively. The TEM photomicrographs [Figure 8(b) and 9(b)] showed evidence of a high intercalation and exfoliation of NC layers in the rubber matrix.

Dynamic Mechanical Investigations

Effects of the Temperature on the Loss Factor and Storage Modulus. Dynamic mechanical analysis is an effective tool for obtaining some indirect evidence on the dispersion of the layered silicate.[28–30] In dynamic mechanical measurements, the storage modulus and tan δ for the filled samples are obtained and plotted against the temperature. The dynamic mechanical properties of the control XHAF 20 with 2.5- and 5-phr CTBN are shown in Figures 10 and 11, respectively. The rubbery modulus did not show any change from that of the control, even after the addition of CTBN, whereas in the glassy state, the modulus showed a decrease after the addition of CTBN. The glass transition process was detectable at -14°C, and T_g remained unaffected by the addition of CTBN. This indicated that although the plasticizing effect was manifested in the rheological and mechanical properties (Tables III and IV), no significant change in T_g due to the addition of CTBN was observed.

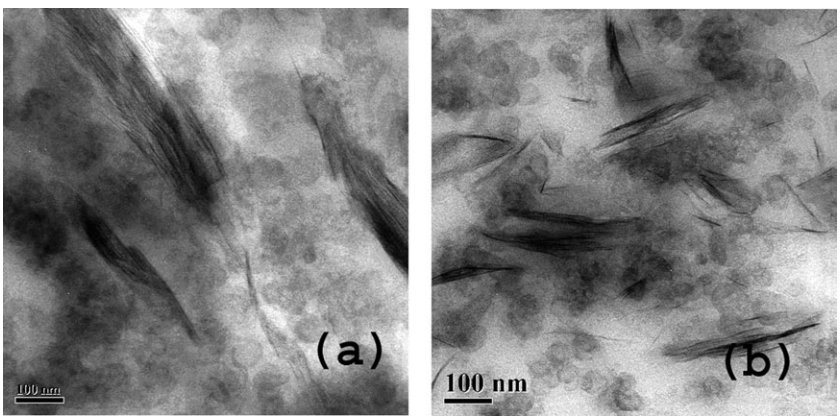

Figure 9. TEM photomicrographs of black-filled XNBR nanocomposites (a) with only NC and (b) with CTBN-modified NC.

Table IV. Tensile Properties of the XNBR Nanocomposites

Composition	Tensile strength (MPa)	Elongation at break (%)	Stress at 100% elongation (MPa)	Stress at 300% elongation (MPa)
XNBR-HAF 20	10.9	374	2	7.4
XCT 2.5	17.5	486	1.9	7.8
XCT 5	18.5	538	1.7	6.5
XNC 2.5	17.7	464	2.1	7.8
XNC 5	15.7	441	2.4	8
XNC 10	9.8	359	2.5	7.7
XNC-CT 2.5	19.5	549	2.1	7.2
XNC-CT 5	24.8	574	2.6	8.8
XNC-CT 10	21.4	554	3	9

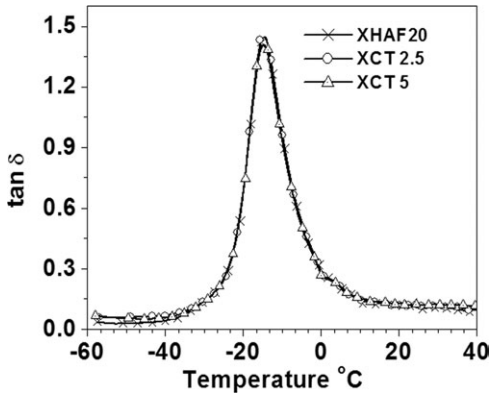

Figure 11. Tan δ as a function of the temperature for XNBR with only CTBN.

The effects of NC on the dynamic properties of XHAF 20 are shown in Figures 12 and 13. The storage modulus increased with increasing NC loading. The modulus increased from 5 MPa (for XHAF 20) to 9 MPa (for XNC 10). At temperatures above the glass-transition temperature, the storage modulus increased significantly. This indicated that NC was more efficient in reinforcing rubber. A similar observation was reported by Ratna[1,2] for epoxy–clay systems. The tan δ_{max} values decreased from 1.4 to 1.18 for XNC 10. This was attributed to an increase in the stiffness resulting from NC incorporation.[29]

With the modification of NC with CTBN, the storage modulus (Figure 14) showed a steady increase with increasing clay loading. This followed a similar trend shown by non-CTBN-modified nanocomposites, as discussed previously. However, as discussed previously for the same amount of NC, the CTBN-modified NC composite system showed a higher rubbery modulus than the non-CTBN-modified system. This showed that the polymer–filler interaction increased after the CTBN modification of NC and led to a higher reinforcing effect. The temperature dependence of tan δ for the CTBN-modified NC composites is shown in Figure 15. The tan δ_{max} values decreased with increasing NC loading. Here again, the magnitude of the decrease was higher in the case of the modified system compared to that of the respective nonmodified systems. This was the result of hindered chain mobility due to higher polymer–filler interactions; this restricted the polymer chain from taking part in the relaxation process and led to lower energy losses.[30]

Dynamic Strain Sweep. The dynamic strain sweep behavior for the XNBR nanocomposites is shown in Figure 16. As observed from the tensile stress values at 100 and 300% elongations (Table IV), the dynamic modulus also showed a similar trend. The CTBN-modified systems showed higher moduli for the same NC loadings. This supported the argument that the mixing of NC with a low-molecular-weight component and their incorporation resulted in better intercalation and polymer–filler interaction on addition to the XNBR matrix.

CONCLUSIONS

A new liquid-rubber-assisted dispersion technique was used to prepare XNBR–clay nanocomposites. The liquid rubber selected was a commercially available CTBN with an acrylonitrile

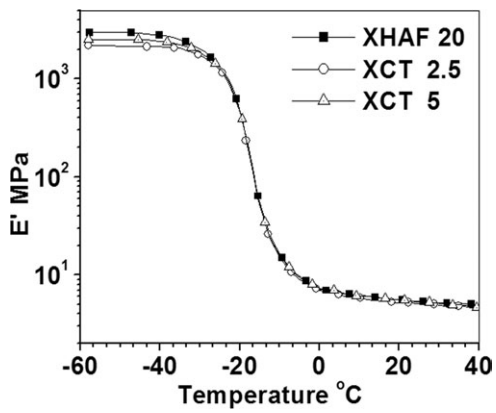

Figure 10. Storage modulus (E') as a function of the temperature for XNBR with only CTBN.

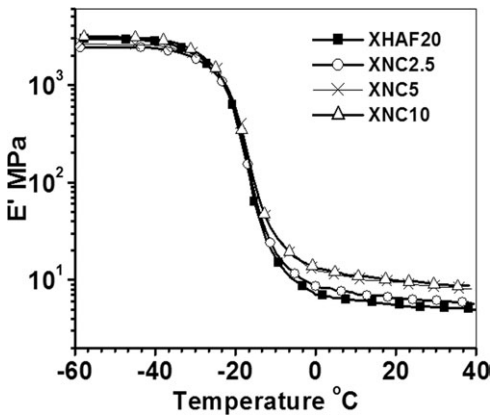

Figure 12. Storage modulus (E') as a function of the temperature for XNBR with only NC.

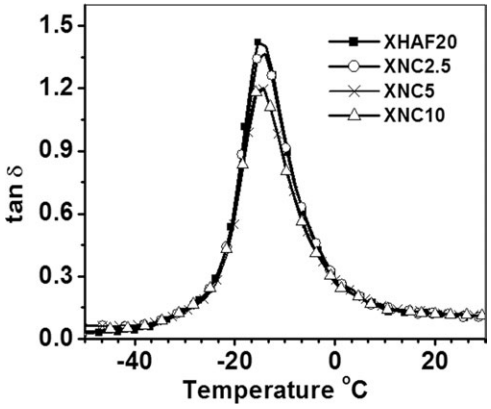

Figure 13. Tan δ as a function of the temperature for XNBR with only NC.

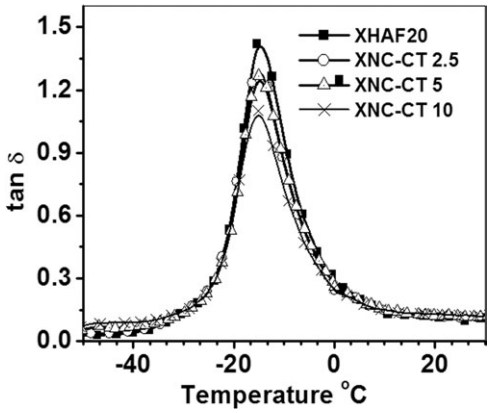

Figure 15. Tan δ as a function of the temperature for XNBR with CTBN-modified NC.

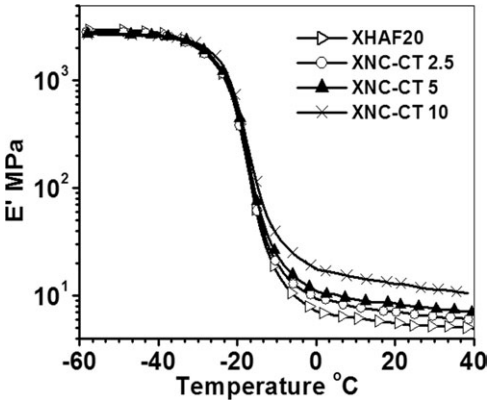

Figure 14. Storage modulus (E') as a function of the temperature for XNBR with CTBN-modified NC.

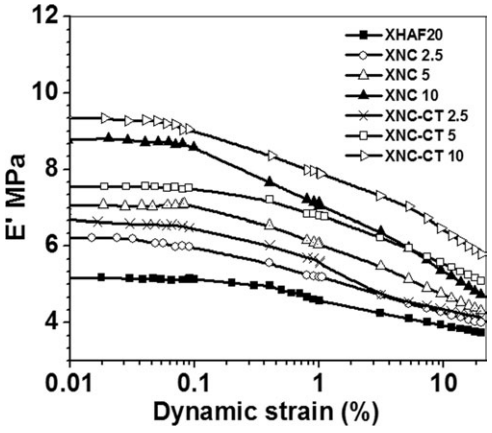

Figure 16. Dynamic strain sweep results for the XNBR nanocomposites (E' = storage modulus).

content of 26% and a number-average molecular weight of 3150. The addition of NC accelerated the curing of the rubber composite. The addition of only liquid rubber to the black-filled system resulted in an increase in the curing time due to a dilution effect. XRD analysis revealed that NC showed additional peaks toward higher angles, which suggested the collapse of the clay layers. This layer collapse was explained by a consideration of the high compressive stress encountered by the clay layers during processing in a two-roll mill. No sign of layer collapse was observed for the CTBN-containing nanocomposite formulations. This was attributed to the penetration of CTBN into the clay galleries during mixing in an internal mixer. The mixing of the pre-expanded clay with XNBR in a two-roll mill resulted in further dispersion without any collapse of the clay layers. XRD analysis of the CTBN-modified clay indicated the exfoliation of clay layers by CTBN and XNBR. However, the TEM analysis indicated a mixed morphology of intercalated and exfoliated structures for nanocomposites made with CTBN-assisted method and a mixture of intercalated layers and tactoids for the nanocomposites made without CTBN. The TEM analysis clearly demonstrated better dispersion of NC as a result of the use of CTBN as a modifier. The mechanical and dynamic mechanical properties were found to be significantly enhanced because of the improvement in the dispersion of the clay as a result of CTBN modification.

REFERENCES

1. Ratna, D. Handbook of Thermoset Resins; Smithers Rapra Technology: London, **2009;** p 410.
2. Ratna, D. *Rapra Rev. Rep.* **2005,** *16*, 1.
3. Jordan, J.; Jacob, I. K.; Tannenbaum, R.; Sharaf, M. A.; Jasiuk, I. *Mater. Sci. Eng. A.* **2005,** *393*(1–2), 1.
4. Ray, S. S. *J. Ind. Eng. Chem.* **2006,** *12*, 811.
5. Vu, Y.; Mark, T. J. E.; Pham, L. H. *J. Appl. Polym. Sci.* **2001,** *82*, 1391.
6. Sadhu, S.; Bhowmick, A. K. *Rubber Chem. Technol.* **2003,** *76*, 860.
7. Sadhu, S.; Bhowmick, A. K. *J. Appl. Polym. Sci.* **2004,** *92*, 698.
8. Karger-Kocsis, J.; Wu, C. M. *Polym. Eng. Sci.* **2004,** *44*, 1083.
9. Wu, Y. P.; Ma, Y.; Wang, Y. Q.; Zhang, L. Q. *Macromol. Mater. Eng.* **2004,** *289*, 890.

10. Paul, D. R.; Robeson, L. M. *Polymer.* **2008,** *49*, 3187.
11. Maiti, M.; Sadhu, S.; Bhowmick, A. K. *J. Appl. Polym. Sci.* **2005,** *96*, 443.
12. Praveen, S.; Chattopadhyay, P. K.; Albert, P.; Dalvi, V. G.; Chakraborty, B. C.; Chattopadhyay, S. *Compos. A* **2009,** *40*, 309.
13. Praveen, S.; Chattopadhyay, P. K.; Jayendran, S.; Chakraborty, B. C.; Chattopadhyay, S. *Polym. Compos.* **2010,** *59*, 187.
14. Dennis, H. R.; Hunter, D. L.; Chang, D.; Kim, S.; White, J. L.; Cho, J. W.; Paul, D. R. *Polymer* **2001,** *42*, 9513.
15. Fornes, T. D.; Yoon, P.; Keskkula, H.; Paul, D. R. *Polymer* **2001,** *42*, 9929.
16. Ray, S. S.; Okamoto, M. *Prog. Polym. Sci.* **2003,** *28*, 1539.
17. Alexandre, M.; Dubois, P. *Mater. Sci. Eng. Rep.* **2000,** *28*, 1.
18. Biswas, M.; Ray, S. S. *Adv. Polym. Sci.* **2001,** *155*, 167.
19. Roberts, A. D. Natural Rubber Science and Technology; Oxford Science: Oxford, United Kingdom, **1990.**
20. Ganter, M.; Gronski, W.; Semke, H.; Zilg, T.; Thomann, C.; Mülhaupt, R. *Kaut. Gummi Kunstst.* **2001,** *54*, 166.
21. Ganter, M.; Gronski, W.; Reichert, P. *Rubber Chem. Technol.* **2001,** *74*, 221.
22. Pramanik, M.; Srivastava, S. K.; Samantaray, B. K.; Bhowmick, A. K. *J. Appl. Polym. Sci.* **2003,** *87*, 2216.
23. Wang, Y.; Zhang, L.; Tang, C.; Yu, D. *J. Appl. Polym. Sci.* **2000,** *78*, 1879.
24. Mousa, A.; Karger-Kocsis, J. *Macromol. Mater. Eng.* **2001,** *286*, 260.
25. Schon, F.; Thomann, R.; Gronski, W. *Macromol. Symp.* **2002,** *189*, 105.
26. Rajasekar, R.; Kaushik, P.; Heinrich, G.; Das, A.; Das, C. K. *Mater. Des.* **2009,** *30*, 3839.
27. Varghese, S.; Karger-Kocsis, J.; Gatos, K. G. *Polymer* **2003,** *44*, 3977.
28. Varghese, S.; Gatos, K. G.; Apostolov, A. A.; Karger-Kocsis, J. *J. Appl. Polym. Sci.* **2004,** *92*, 543.
29. Schön, F.; Gronski, W. *Kaut. Gummi Kunstst.* **2003,** *56*, 166.
30. Lu, H. B.; Nutt, S. *Macromolecules* **2003,** *36*, 4010.